DOI 10.1007/s10778-015-0711-9
International Applied Mechanics, Vol. 51, No. 5, September, 2015

NUMERICAL ANALYSIS OF THE EDGE EFFECT IN A COMPOSITE LAMINATE WITH COMPRESSED REINFORCEMENT PLIES

V. M. Bystrov, V. A. Dekret, and V. S. Zelenskii

A piecewise-homogeneous material model is used to numerically determine the edge effect length in a composite laminate with reinforcement plies subject to unidirectional longitudinal compression. Consideration is given to mixed boundary conditions (regularity of the material structure and symmetry of the surface load) on the sides of the composite specimen and boundary conditions for stresses on the stress-free sides of the specimen. The dependence of the edge effect length on the ratio of the mechanical characteristics of the composite components is studied

Keywords: composite laminate specimen, compression of reinforcement plies, edge effect length, modified variational difference method

Introduction. In designing and testing composite materials (CMs), it is of interest to analyze the combined effect of such factors as the structural inhomogeneity of a CM and the loading and boundary conditions of a CM specimen on the edge effects. One of the aspects of this problem is the analysis of the zone of unsteady stress–strain state (edge effect) where a surface load that changes substantially at distances comparable with the typical length scale of the structural inhomogeneity of the CM is applied. This, in particular, represents the case where a surface load is applied only to the reinforcement of a CM specimen. In many studies on the influence of the inhomogeneity of a material on the decay of edge effects, it is pointed out that the edge effect length may be rather great at a certain ratio of the elastic and geometrical characteristics of the composite components [1, 8, 12, 13, 15, 17–20]. This strongly restricts the conventional application of Saint Venant's principle in designing structures made of CMs. The way the edge effect decays, the geometry of its zone, and the distribution of stresses and strains in the edge effect zone depend on the ratio of the sizes of the region of variation in the external load and the structural inhomogeneity of the material. For example, edge effects in unidirectional fiber-reinforcement composites of regular structure associated with the redistribution of the external load between the matrix and the fibers subject to longitudinal tension were analyzed in [4]. The problem was formulated for a periodicity cell in a hexagonal model of the microstructure. It was shown that the edge effect size is on the order of one to two typical length scales of the internal structure of a CM. Similar results were obtained in [2, 3] for a two-layer periodicity cell of a CM with uniformly loaded reinforcement. As shown in [1, 12], the edge effect zone is much larger if the size of the periodicity cell is determined by the period of the surface load and exceeds the typical length scale of the internal structure of the CM. The asymptotic dependence of the edge effect length on the size of the periodicity cell along the line of application of the surface load allows us to isolate a representative element of the material [8]. A representative element inherits the structure of an inhomogeneous material at a certain scale. For such an element, the dependence of the way the edge effect decays on the geometrical and mechanical characteristics of the CM components is not affected by the choice of a computational domain.

In [1, 12], a piecewise-homogeneous material model, equations of elasticity, and a quantitative decay criterion were used to analyze the decay of the edge effect in a laminated CM under uniaxial longitudinal piecewise-constant compressive load applied to the reinforcement plies. The dependence of edge effect decay parameters on the period of the surface load was analyzed. The change in the period of the load was associated with the change in the number of non-loaded plies. It was shown

S. P. Timoshenko Institute of Mechanics, National Academy of Sciences of Ukraine, 3 Nesterova St., Kyiv, Ukraine 03057, e-mail: numer@inmech.kiev.ua. Translated from Prikladnaya Mekhanika, Vol. 51, No. 5, pp. 90–98, September–October 2015. Original article submitted December 25, 2013.

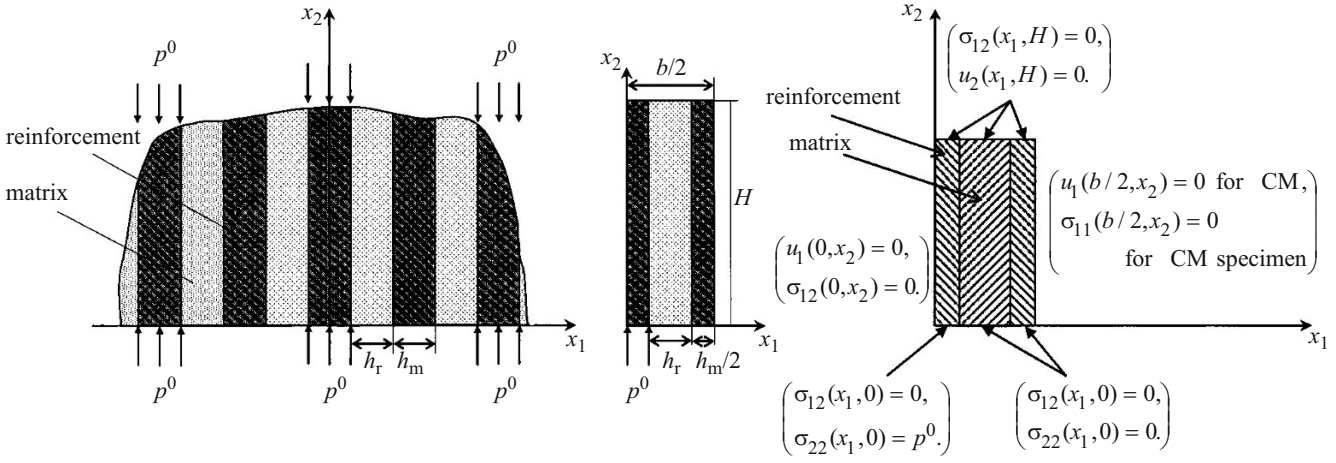

a *b* *c*

Fig. 1

that one non-loaded reinforcement ply in the computational domain makes the major contribution to the increase in the edge effect length upon a change in the spatial period of the surface load, which corresponds to a load period equal to two spatial periods of the material. The edge effect length is maximum in the non-loaded reinforcement ply. Further increase in the period of the surface load caused the edge effect length to slightly increase (within 5%), tending to a constant value. Thus, in studying edge effects, it is reasonable to use, as a representative element of the material, a computational domain whose length along the load application line is equal to two spatial periods of the structure.

Here we will use such a computational domain to construct a design model and to analyze the influence of the elastic characteristics of the components of a laminated CM on the decay behavior of the edge effect for two types of boundary conditions on the sides of the domain. One type of boundary conditions corresponds to symmetry for a periodicity cell of an infinite laminated material, and the other type to stress-free sides of a composite specimen. In what follows, we will associate the former type of boundary conditions with the CM, while the latter type with a CM specimen that has a finite dimension along the line of application of the surface load. Analyzing various boundary conditions allows a more adequate description of the real service conditions of composites. Similar design models were used in [10] to determine and analyze the inhomogeneous subcritical state in a stability problem. Among few studies related to the influence of inhomogeneity on the decay of edge effects for such boundary conditions (the so-called Dirichlet and Neumann boundary conditions), the papers [8, 17] are noteworthy.

Using various methods to analyze edge effects, including the eigensolution method, the method of energy inequalities, etc., in most cases produces bound estimates for the edge effect length [8, 13, 17–20], providing no answers to the questions on the geometry of the edge effect zone and the distribution of stresses and strains in it.

We will use the equations of elasticity for inhomogeneous bodies and quantitative criteria for the estimation of the edge effect [2, 3]. Such an approach will allow us to obtain the fullest information on the decay of the edge effect where a surface load is applied.

Since it is difficult to find analytic solutions to problems of this class, modern numerical methods have to be used [5, 6]. The numerical approach to be used to analyze the edge effect and stability of fibrous and laminated composites in inhomogeneous subcritical states was developed in [1, 7, 10–12]. It is a modified variational difference approach that employs a mesh-based method and the concept of reference difference scheme [11]. The conventional variational difference approach and its applications to structural members made of CMs are addressed, for example, in [14].

1. Problem Formulation. Design Models. Let us determine the edge effect length in a two-component CM of regular structure with reinforcement plies subject to a uniaxial compressive surface load of constant intensity with spatial period equal to two spatial periods of the CM (Fig. 1*a*). At infinity, the reinforcement plies are assumed to be compressed by a load of the same spatial period. Since the load is symmetric and the structure of the CM is regular, the problem can be solved using a finite computational domain (Fig. 1*b*). Since we are to analyze the influence of the boundary conditions on the sides of the computational domain on the decay of the edge effect, we will distinguish a composite and a specimen made of this composite. In the former case, the boundary conditions on the sides of the model are symmetry conditions. In the latter case, the sides of the

specimen are free from stresses. Let the former design model correspond to the material, and the latter model to the specimen. Thus, we will use two design models to compare the decay of the edge effect in the material under various boundary conditions for the specimen (Fig. 1*c*).

In formulating the problem, we will use a Cartesian coordinate system $Ox_1x_2x_3$ and place the CM and CM specimen in the upper half-space $x_2 \geq 0$. Let the plies extend along the Ox_3-axis, be parallel to the plane Ox_2x_3, and let the reinforcement plies be compressed along the Ox_2-axis by a surface load of constant intensity. If these conditions are satisfied, the problem can be formulated as two-dimensional for plane strain in the plane x_1Ox_2 (Fig. 1, which shows the geometry of the computational domain and the loading conditions).

The design models used here include boundary-value problems of elasticity for piecewise-homogeneous bodies and a quantitative criterion of decay of edge effect for normal stresses [1, 12]. When a layered material is deformed longitudinally so that the edge effect extends along continuous layers, the stresses vary monotonically, and the stress state in each component of the material becomes homogeneous after the decay of the edge effect. The steady-state normal stresses are used in the criterion of decay of edge effect. The design models for the CM and CM specimen differ by the boundary conditions on the side $x_1 = b/2$ (mixed homogeneous conditions and homogeneous conditions for stresses (Fig. 1*c*)).

The surface load p acts along the Ox_2-axis and is applied to the reinforcement plies: $p(x_1) = \sigma_{22}(x_1, 0) = p^0$, $|x_1| \leq 0.5h + kb$, $k = 0, 1, \ldots$. The spatial period b of the surface load is equal to two spatial periods of the composite structure: $b = 2h$, $h = h_r + h_m$, where h_r and h_m are the thicknesses of the reinforcement and matrix plies, respectively. The load does not vary along the Ox_3-axis. Since the layered structure is regular and the surface load is periodic, the computational domain $\overline{\Omega}$ can be represented as follows:

$$\overline{\Omega} = \bigcup_{n=1}^{2} \overline{\Omega}^{(n)} = \{(x_1, x_2) | 0 \leq x_1 \leq b/2,\ 0 \leq x_2 \leq H\}, \tag{1.1}$$

where $\overline{\Omega}^{(n)}$ is the domain occupied by the structural element n of the material. This element is formed by halves of neighboring plies of reinforcement and matrix and its size along the Ox_2-axis is $h/2$. The size of the computational domain along the Ox_1-axis is equal to half the period b of the surface load. The size H of this domain along the Ox_2-axis is determined in a computational experiment from the conditions that the stress state can be considered steady with prescribed accuracy along the Ox_2-axis and that the decay behavior of the edge effect is independent of this size. The following formula holds for the geometrical parameters of the material and the load parameters: $h_r < h \leq b < H$.

The boundary conditions on the section $\{0 \leq x_1 \leq b/2, x_2 = 0\}$ of the boundary of the computational domain $\overline{\Omega}$ determine the surface load. The boundary conditions on the sections $\{x_1 = 0, 0 \leq x_2 \leq H\}$ and $\{x_1 = b/2, 0 \leq x_2 \leq H\}$ express the periodicity of the stress state and symmetry and are mixed homogeneous conditions for the CM. The same conditions, following from symmetry, are set on the section $\{x_1 = 0, 0 \leq x_2 \leq H\}$ for the CM specimen. The boundary conditions on the section $\{x_1 = b/2, 0 \leq x_2 \leq H\}$ of the boundary of the computational domain are homogeneous conditions for stresses. The boundary conditions on the section $\{0 \leq x_1 \leq b, x_2 = H\}$ prohibit rigid-body displacement and rotation of the computational domain and are mixed homogeneous conditions as well.

To determine the boundary $\Gamma_\rho(x_1, x_2)$ and decay length λ_ρ of the edge effect with an error ρ%, we will use the following conditions:

$$\widetilde{\rho}(x_1, x_2)\big|_{x \in \Gamma_\rho} = \rho \tag{1.2}$$

$$(\widetilde{\rho} = 100(\sigma(x) - \sigma_{st})/(p(x_1, 0) - \sigma_{st}), \quad x = (x_1, x_2) \in \Gamma_\rho)$$

for a composite laminate under longitudinal compression.

Here $\sigma_{st} = \sigma(x_1, H)$ are the steady-state stresses on the boundary $x_2 = H$ of the computational domain in the direction of decay of the edge effect; $p(x_1) = \sigma(x_1, 0)$ is the surface load on the boundary $x_2 = 0$ of the computational domain; $\sigma(x) = \sigma_{22}(x)$.

The decay length λ_ρ of the edge effect is determined as the maximum length of the edge effect in the direction of its decay:

$$\lambda_\rho = \max_{x_1, x_2 \in \Gamma_\rho} (x_2). \tag{1.3}$$

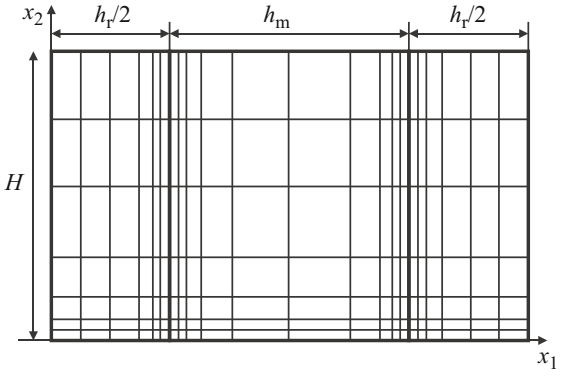

Fig. 2

2. Numerical Solution of the Problem. Mesh-Based Method. To determine the stress state, we will use a criterion of decay of the edge effect and the mesh-based method based on the modified variational difference approach [11]. With such an approach, the difference scheme for the computational domain is constructed at each node as a sum of values of the reference scheme, which is a difference scheme obtained by a variational difference method for the cell template of the difference mesh.

For numerical purposes, the problem for the original semi-infinite model of the composite is reduced to a problem for a finite computational domain. The size of this domain is determined in a computational experiment from the condition that the maximum edge effect length no longer changes with increase in the dimension of the domain along the Ox_2-axis. The sizes of the computational domain for the CM are also used for the CM specimen when comparing the influence of the boundary conditions on the decay of the edge effect.

Figure 2 shows the computational domain covered by a nonuniform difference mesh. Over the rectangular nonuniform difference mesh $\overline{\omega} = \omega + \gamma$, which approximates the domain $\overline{\Omega}$, the continuous problem is associated with the following difference problem:

$$L_{im}\, y(x) = F_{im}(x), \qquad x = (x_1, x_2) \in \overline{\omega} \tag{2.1}$$

$$\left(L_{im}(x) = \begin{cases} \sum\limits_{\xi \in x} a_{im}(x) y_i, & x \in y_{im} \\ y_m, & x \in y_{im} \end{cases}; \quad F_{im} = \begin{cases} \sum\limits_{\xi \in x} \varphi_{im}(\xi) y_m; \\ Y_m \end{cases} \right.$$

$$a_{im}(\xi) y_i = \begin{cases} -h \dfrac{\tau_{im} + \tau_{im}^{-\xi_i}}{\eta_{\xi_i}}, & \xi \in s_{\sigma_{im}} \\ y_m, & \xi \in s_{y_m} \end{cases}; \quad \varphi_m(\xi) = \begin{cases} h\left(F_{im} + 2\dfrac{P_{im}}{\eta_{\xi_i}} \right); \\ Y_m \end{cases}$$

$$\left. \tau_{ii} = A_{ik} e_{kk}, \;\; \tau_{12} = 2G e_{12}, \;\; e_{ij} = 0.5(y_{i,\xi_j} - y_{j,\xi_i}), \;\; y_{i,\xi_j} = -\operatorname{sign}(\xi_i) \frac{y_i^{-\xi_j} - y_i}{h_{\xi_i}} \right), \tag{2.2}$$

where τ_{ij}, e_{ij}, y_m are difference analogs of the continuous variables $\sigma_{ij}, \varepsilon_{ij}, u_m$; a_{im}, φ_m are the components of the reference operator a and reference function φ; H is the cell area; $\eta_i = -\operatorname{sign}(\xi_j) \cdot h_{\xi_i}$ is the alternating-sign pitch; $h_{\xi_i} = -\operatorname{sign}(\xi_j)\eta_{\xi_i} > 0$ is the constant-sign pitch; $h_{\xi_i} = h_{-\xi_i} = h_j > 0$ since the sign is constant; y_{i,ξ_j} is the difference derivative of the mesh function $y(\xi)$ in the x_i-direction (right derivative for $\xi_i < 0$); $\xi = (\xi_1, \xi_2)$, $\xi_i = \pm i$ is the node parameter of the cell; $\sum_{\xi \in x}$ denotes the summation of a component of the reference scheme over those parameters ξ that coincide with the mesh node x; $\xi_{-i} = -\xi_i$; E is an identity operator, γ_{u_m} is the section of the boundary γ on which the mth component of the difference analog of the boundary condition is set for displacements.

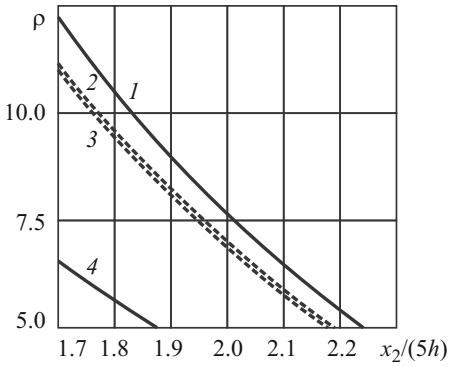

Fig. 3

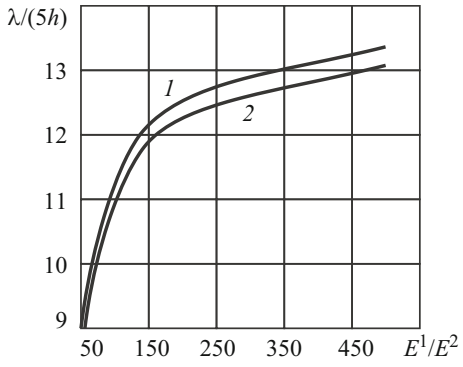

Fig. 4

The difference problem is solved with the direct Cholesky method followed by the application of the conjugate-gradient method [15]. The solution is found by the former method and is then used as the initial approximation in the latter method. The difference mesh is refined by halving its pitch on the boundaries of the computational domain and at the interfaces between the CM components.

3. Analysis of the Numerical Results. Consider a CM and a CM specimen with identical computational domains and the following mechanical and geometric characteristics: E^1 / E^2 = 20, 50, 100, 200, 500 GPa, $\nu^1 = \nu^2 = 0.3$, $c_r = h_r / (h_r + h_m) = 0.5$, $p^0 = 1$ GPa. Here E^1, ν^1 and E^2, ν^2 are, respectively, Young's moduli and Poisson's ratios of the reinforcement and matrix; $c_r = 0.5$ is the volume fraction of the reinforcement, where h_r and h_m are, respectively, the thicknesses of the reinforcement and matrix plies; p^0 is the intensity of the surface load with period $b = 2h$, $h = h_r + h_m$, applied to reinforcement plies.

Calculations show that the edge effect is the largest in the contact area $x_1 = h_r / 2 + h_m$ between the reinforcement ply and the non-loaded reinforcement ply. Figure 3 shows the behavior of the decay function defined by (1.1), (1.2) for E^1 / E^2 = 100. Curves *1* and *2* correspond to the CM specimen, and curves *3* and *4* to the CM. With the boundary conditions for stresses on the boundary $x_1 = b / 2$ in the CM specimen, the edge effect decays slower than with the mixed boundary conditions in the CM. In the CM specimen, the edge effect decays faster in the matrix (curve *2*) than in the reinforcement (curve *1*). In the CM, the edge effect decays faster in the reinforcement (curve *4*) than in the matrix (curve *3*). That is, different boundary conditions have different effects on the stress distribution between the reinforcement and the matrix and, hence, on the way the edge effect decays in the reinforcement and the matrix.

Figure 4 shows the variation in the maximum edge effect length in the CM (curve *2*) and the CM specimen (curve *1*) with E^1 / E^2. The edge effect length $\lambda = \lambda_\rho$ has been determined with error $\rho = 5\%$ according to (1.3). For illustrative purposes, the edge effect length is divided by 5*h*. The graphs display a qualitatively similar behavior for the CM and the CM specimen. The maximum edge effect length in the CM specimen is greater than in the CM over the entire range of variation in the ratio of Young's moduli of the reinforcement and the matrix and the difference is greater at greater values of this ratio.

The results indicate that the mixed boundary conditions on the sides of the computational domain (symmetry conditions and kinematic conditions for one of the components) reduce the edge effect length. Thus, the design models used above for comparative analysis of the decay of the edge effect in the CM specimen and the CM allow for the effect of the boundary conditions on the mechanisms of redistribution of the external load between the reinforcement and the matrix and allow a more adequate description of the effect of real service conditions of structural members and test conditions for CM specimens on these mechanisms.

Conclusions. We can now draw the following conclusions.

The edge effect length near the area of application of a surface load in the CM specimen with boundary conditions for stresses on the sides of the computational domain exceeds that in the CM with mixed boundary conditions. The redistribution of the external load between the reinforcement and the matrix for different boundary conditions leads to opposite maximum edge effect lengths in the components of the CM and CM specimen: the edge effect length is maximum in the reinforcement of the CM specimen and is maximum in the matrix of the CM.

As the ratio of Young's moduli of the CM components is increased, which means stronger anisotropy of the material at macromechanical level, the maximum edge effect length increases in both the CM and the CM specimen.

The mixed boundary conditions on the sides of the computational domain (symmetry conditions and kinematic conditions for one of the components) reduce the edge effect length.

REFERENCES

1. V. M. Bystrov and V. S. Zelenskii, "Decay of the edge effect in materials reinforced with rectangular components and subject to longitudinal and transverse compression," in: *Systems Technologies* [in Ukrainian], Issue 3(62), Dnipropetrovsk (2009), pp. 99–104.
2. V. T. Golovchan, A. N. Guz, Yu. V. Kokhanenko, and V. I. Kushch, *Statics of Materials*, Vol. 1 of the 12-volume series *Mechanics of Composite Materials* [in Russian], Naukova Dumka, Kyiv (1993).
3. Ya. M. Grigorenko, Yu. N. Shevchenko, A. T. Vasilenko, et al., *Numerical Methods*, Vol. 11 of the 12-volume series *Mechanics of Composite Materials* [in Russian], A.S.K., Kyiv (2002).
4. I. V. Andrianov, V. V. Danishevs'kyy, and D. Weichert, "Analytical study of the load transfer in fiber-reinforced 2D composite materials," *Int. J. Solids Struct.*, **45**, 1217–1243 (2008).
5. J. E. Akin, *Finite Element Analysis Concepts: via SolidWorks*, World Scientific, Hackensack, NJ (2010).
6. E. J. Barbero, *Finite Element Analysis of Composite Materials Using ANSYS*, CRC Press, Taylor & Francis Group (2013).
7. E. Yu. Bashchuk and V. Yu. Baichuk, "Influence of the principal stress state on the critical loads of a plate with a crack," *Int. Appl. Mech.*, **49**, No. 3, 328–336 (2013).
8. S. C. Baxter and C. O. Horgan, "End effects for anti-plane shear deformation of sandwich structure," *J. Elasticity*, **40**, No. 2, 123–164 (1995).
9. V. M. Bystrov, "Analysis of the decay of edge effects in laminated materials on the basis of representative element," *Int. Appl. Mech.*, **36**, No. 6, 826–835 (2000).
10. V. A. Dekret, V. S. Zelenskii, and V. M. Bystrov, "Numerical analysis of the stability a laminated composite with uniaxially compressed reinforcement plies," *Int. Appl. Mech.*, **50**, No. 5, 549–557 (2014).
11. Yu. V. Kokhanenko, "Numerical analysis of edge effects in laminated composites under uniaxial loading," *Int. Appl. Mech.*, **46**, No. 5, 516–529 (2010).
12. Yu. V. Kokhanenko and V. M. Bystrov, "Edge effect in a laminated composite with longitudinally compressed laminas," *Int. Appl. Mech.*, **42**, No. 8, 922–928 (2006).
13. M. C. Leseduarte and R. Quintanilla, "Saint-Venant decay rates for a non-homogeneous isotropic mixture of elastic solids in anti-plane shear," *Int. J. Solids Struct.*, **42**, No. 9–10, 2977–3000 (2005).
14. V. A. Maksimyuk, E. A. Storozhuk, and I. S. Chernyshenko, "Variational finite-difference methods in liner and nonliner problems of the deformation of metalic and composite shells (review)," *Int. Appl. Mech.*, **48**, No. 5, 613–687 (2012).
15. K. L. Miller and C. O. Horgan, "Saint-Venant end effects for plane deformations of elastic composites," *Mech. Comp. Mater. Struct.*, **2**, No. 3, 203–214 (1995).
16. S. Pissanetzky, *Sparse Matrix Technology*, Academic Press, London (1984).
17. M. R. Scalpato and C. O. Horgan, "Saint-Venant decay rates for an isotropic inhomogeneous linearly elastic solid in anti-plane shear," *J. Elasticity*, **48**, No. 2, 145–166 (1998).
18. N. Tullini and M. Savoia, "Decay rate of Saint-Venant end effects for multilayered orthotropic strips," *Int. J. Solids Struct.*, **34**, No. 33–34, 4263–4280 (1997).
19. A. C. Wijeyewickrema, "Decay of stresses induced by self-equilibrated end loads in a multilayered composite," *Int. J. Solids Struct.*, **32**, 515–523 (1995).
20. A. C. Wijeyewickrema, C. O. Horgan, and J. Dundurs, "Further analysis of end effects for plane deformations of sandwich strips," *Int. J. Solids Struct.*, **33**, 4327–4336 (1996).